



1 **Measurement Report: Polycyclic aromatic hydrocarbons (PAHs) and their**
2 **alkylated (RPAHs), nitrated (NPAHs) and oxygenated (OPAHs) derivatives in**
3 **the global marine atmosphere: occurrence, spatial variations, and source**
4 **apportionment**

5 Rui Li^{a,b}, Yubing Shen^a, Yumeng Shao^a, Yining Gao^a, Ziwei Yao^c, Qian Liu^c, Xing Liu^{c,*}, Guitao
6 Shi^{a,*}

7 ^a *Key Laboratory of Geographic Information Science of the Ministry of Education, School of*
8 *Geographic Sciences, East China Normal University, Shanghai, 200241, PR China*

9 ^b *Institute of Eco-Chongming (IEC), 20 Cuiniao Road, Chenjia Town, Chongming District,*
10 *Shanghai, 202162, China*

11 ^c *State Environmental Protection Key Laboratory of Coastal Ecosystem, National Marine*
12 *Environmental Monitoring Center, Dalian 116023, China*

13 *** Corresponding author**

14 Prof. Liu (xliu@nmemc.org.cn) and Prof. Shi (gtshi@geo.ecnu.edu.cn)

15 **Abstract**

16 Ambient polycyclic aromatic hydrocarbons (PAHs) and their derivatives have severe adverse
17 impacts on organism health and ecosystem safety. However, their global distributions, sources, and
18 fate in marine aerosols remain poorly understood. To fill the knowledge gap, high-volume air
19 samples were collected along a transect from China to Antarctica and analyzed for particulate PAHs
20 and derivatives. The highest PAH concentrations in marine aerosols were observed in the Western
21 Pacific (WP: 447±228 pg/m³), followed by the East China Sea (ECS: 195 pg/m³), Antarctic Ocean
22 (AO: 111±91 pg/m³), East Australian Sea (EAS: 104±88 pg/m³), and the lowest in the Bismarck Sea
23 (BS: 17±12 pg/m³). Unexpectedly, PAH concentrations in the AO were even higher than those in
24 the EAS and BS. This could be attributed to the relatively low anthropogenic PAH emissions from
25 Australia and Papua New Guinea, whereas AO is often affected by emissions from engine
26 combustion and biomass burning. In contrast to the distribution of PAHs, OPAH levels in the EAS
27 were much higher than those in the AO. It was assumed that OPAHs mainly originated from the
28 secondary formation of parent PAHs through reactions with O₃ and OH radicals, both of which are
29 more prevalent in EAS. Several source apportionment models suggested that PAHs and their



30 derivatives in marine aerosols are dominated by three sources: coal burning and engine combustion
31 emissions (56%), wood and biomass burning (30%), and secondary formation (14%). Specifically,
32 marine aerosols in ECS and WP were significantly affected by coal burning and engine combustion,
33 while those in BS and EAS were mainly influenced by wildfire and coal combustion. AO was
34 primarily dominated by biomass burning and local shipping emissions.

35 **1. Introduction**

36 Polycyclic aromatic hydrocarbons (PAHs), a class of semi-volatile organic compounds
37 (SVOCs), are often considered carcinogenic and mutagenic pollutants (Li et al., 2023; Wei et al.,
38 2021). These pollutants are generally released from the combustion of fossil fuels, biofuels, oil spills,
39 and other biogenic sources (Li et al., 2021a; Zhang et al., 2023). Due to long-range atmospheric
40 transport (LRAT), PAHs emitted from industrial and residential sources can often be transported to
41 remote regions such as the open ocean and polar areas (Li et al., 2021a; Zhang et al., 2023). These
42 PAHs species can exert toxic effects on marine organisms through dry and wet deposition (Li et al.,
43 2021b). Additionally, high levels of oxidants (OH radicals, NO₃ radicals, and O₃) enriched in the
44 atmosphere can promote the transformation of parent PAHs into their derivatives (RPAHs, NPAHs,
45 and OPAHs) (Zimmermann et al., 2013). Compared to parent PAHs, nearly all of these derivatives
46 exhibit higher toxic potency to aquatic animals due to their direct-acting mutagenicity (Bandowe
47 and Meusel, 2017; Kovacic and Somanathan, 2014). Therefore, it is crucial to investigate the
48 spatiotemporal characteristics of PAHs and their derivatives and to identify the key factors and
49 potential sources of atmospheric PAHs. This knowledge is essential for reducing potential damage
50 to ocean ecosystems and improving marine environmental management.

51 A growing body of researches have explored the spatial variations of ambient PAHs in the
52 marine atmosphere. For instance, Kang et al. (2017) found that atmospheric PAH concentrations in
53 the East China Sea ranged from 0.16 to 17.6 ng/m³ (average: 3.87 ng/m³), with these compounds
54 being dominated by 4-ring PAHs. Subsequently, Neroda et al. (2020) investigated PAHs in the
55 aerosols of the North-West Pacific Ocean, estimating total PAH levels ranging from 17.1 pg/m³
56 (northern part of the Sea of Japan) to 142 pg/m³ (La Perouse Strait). More recently, Wietzorek et
57 al. (2022) reported that the mean concentrations of total PAHs, RPAHs, OPAHs, and NPAHs in the
58 gas and particulate phases in the Mediterranean were 2.99 ± 3.35 ng/m³, 0.83 ± 0.87 ng/m³,



59 $0.24 \pm 0.25 \text{ ng/m}^3$, and $4.34 \pm 7.37 \text{ pg/m}^3$, respectively. Most current studies about PAHs in marine
60 aerosols focus on regional scales, particularly in seas with dense anthropogenic activities, while few
61 studies reveal the spatial distributions of PAHs and their derivatives in remote seas (e.g., the polar
62 oceans) or on a global scale. The Southern Ocean is often considered a remote and pristine sea, and
63 its local ecosystem is more sensitive to PAHs and their derivatives. However, to date, only a few
64 studies have investigated the spatial variations of ambient PAHs in the marine aerosols within this
65 region. Cabrerizo et al. (2014) first demonstrated that the volatilization of soils and snows might be
66 the major sources of ambient PAHs in the Southern Ocean and Antarctic. Very recently, Overmeiren
67 et al. (2024) analyzed the components of PAHs and OPAHs at a coastal site in Antarctica and found
68 that phenanthrene, pyrene, and fluoranthene derived from volcanic emissions accounted for the
69 major fractions of PAHs. To the best of our knowledge, only Zhang et al. (2022) investigated the
70 global variations of PAH components in marine aerosols and found a clear latitudinal gradient from
71 the Western Pacific to the Southern Ocean. They also identified coal combustion as the major
72 contributor to ambient PAHs (52%). Unfortunately, nearly all current studies focus solely on PAHs
73 and OPAHs in regional oceans simultaneously, whereas no study has comprehensively investigated
74 the spatial variations of particulate PAHs and all their derivatives on a global scale. Moreover, the
75 source contributions of PAH derivatives in different oceans remain unknown. It is highly necessary
76 to fill the knowledge gaps regarding the compositions, sources, and fate of PAH derivatives in the
77 marine atmosphere on a global scale.

78 In our study, an expedition research cruise aboard a Chinese research vessel from October 2019
79 to April 2020, traveling from China to Antarctica, provided a unique opportunity to reveal the
80 distributions, compositions, and fate of parent PAHs and their derivatives (RPAHs, NPAHs, and
81 OPAHs). Taking advantage of this unique opportunity, our study aims to: (1) investigate the
82 latitudinal gradient of PAHs and their derivatives; (2) study the major factors contributing to the
83 spatial variations; and (3) identify the sources using a Positive Matrix Factorization (PMF) model.

84 **2. Material and methods**

85 2.1 The shipping cruise and sample collection

86 The expedition research cruise of Chinese research vessel took place from October 22 in 2019
87 to April 21 in 2020. The expedition sailed from Shanghai in China, crossing Pacific, Indian Ocean,



88 and Southern Ocean and finally arrived at Antarctic. Then, the return route was also from Antarctic
89 to Shanghai, in China. The detailed information of shipping line is depicted in Figure S1 and 1.

90 Atmospheric samples were collected using a high-volume air sampler (HVAS, TISCH
91 Environmental, USA), positioned on the upper deck of the RV/Xuelong, approximately 30 m above
92 sea level. Aerosol particles were captured on Whatman quartz fiber filters (QM-A, 20.3 cm × 25.4
93 cm, pore size 2.5 μm), which were pre-baked at around 500 °C for over 4 hours to eliminate water
94 and organic residues. The HVAS operated at an airflow rate of approximately 1.2 m³ min⁻¹, with
95 each sampling event lasting 2 to 3 days, resulting in total air volumes typically ranging from 3000
96 to 4000 m³. During this time, atmospheric particles were collected along the cruise path, spanning
97 approximately 2 to 4 degrees of latitude, yielding a single aggregate sample per filter. To minimize
98 potential contamination from the research vessel, a wind direction sensor directed the HVAS,
99 ensuring that only air masses from a sector of approximately 120° on either side of the vessel's
100 central trajectory were sampled. After collection, individual filters were carefully separated, folded,
101 wrapped in aluminum foil, placed in zip-lock bags, and stored in the dark at -20 °C until particle
102 characterization analyses began. A total of 35 samples were collected during the cruise, along with
103 2 field blank samples prepared from filters mounted in the HVAS with an air pump flow rate set to
104 0. The sampling protocols for the blanks mirrored those described above regarding duration, filter
105 mounting, collection, transport, observation, and measurements.

106 2.2 Chemical analysis

107 Automated Soxhlet extraction with DCM (JT Baker, Avantor group, Poland), pesticide residue
108 grade) in a B-811 extraction unit (Büchi, Flawil, Switzerland) for PAH, NPAH, and OPAH analysis
109 was employed. The extract was cleaned up using a silica column (with 1 cm i.d. as open tube using
110 5 g of silica (Merck, Darmstadt, Germany), 0.063-0.200 mm, activated at 150 °C for 12 h, 10%
111 deactivated with water) and 1 g Na₂SO₄ (Merck, Darmstadt, Germany). For the analysis of RPAHs,
112 PM_{2.5} samples were extracted based on the procedure described in Iakovides et al. (2021). A gas
113 chromatograph (Agilent 7890B GC) coupled with the mass spectrometer (Agilent 5977B MS) was
114 employed to determine the concentrations of PAH, NPAH, and OPAH species. The detailed analysis
115 method and quality control of these PAHs and their derivatives are introduced in the supporting
116 information (Text S1 and Table S1).



117 2.3 Source apportionment

118 As a typical receptor-based model used for source apportionment, the PMF 5.0 version have
119 been widely applied to determine the potential origins of PAH and their derivatives, and to determine
120 the contribution ratios of multiple sources to these components (Sharma et al., 2016). The aim of
121 PMF model is to solve the issues of chemical mass balance between the observed concentration of
122 each PAH species and their source contributions via decomposing the input matrix into factor
123 contributions and factor profiles. The detailed equation is shown in Eq. (1). Additionally, the
124 contribution of each source for an individual component should be ensured to be non-negative.
125 Briefly, the basic principle of PMF is to determine the least object function Q when the g_{ik} must be
126 a non-negative matrix based on Eq. (2) (Jaeckels et al., 2007; Taghvaei et al., 2018).

$$127 \quad x_{ij} = \sum_{k=1}^p g_{ik} f_{kj} + e_{ij} \quad (1)$$

$$128 \quad Q = \sum_{i=1}^n \sum_{j=1}^m \left[\frac{x_{ij} - \sum_{k=1}^p g_{ik} f_{kj}}{u_{ij}} \right]^2 \quad (2)$$

129 where x_{ij} and e_{ij} represent the PAH concentrations and uncertainty of the j th component, respectively.
130 g_{ik} denotes the contribution ratio of the k th source to the i th sample, f_{kj} is the ratio of the j th component
131 in the k th source, and e_{ij} denotes the residual of the j th element in the i th sample. The uncertainties
132 linked with factor profiles were assessed based on three error calculation methods including the
133 bootstrap (BS) method, displacement (DISP) analysis, and the combination method of DISP and BS
134 (BS-DISP). For the BS method, 1000 runs were conducted and the result has been considered to be
135 robust because all of the factors showed a mapping of above 90%. DISP analysis also demonstrated
136 that this solution was stable because the observed drop in the Q value was $< 0.1\%$ and no factor
137 swap occurred. For the BS-DISP analysis, the solution has been verified to be useful because the
138 observed drop in the Q value was $< 0.5\%$. Moreover, both of the results from BS and BS-DISP did
139 not show any asymmetry or rotational ambiguity for all of the factors (Ambade et al., 2023; Gao et
140 al., 2015; Yan et al., 2017).

141 2.4 GEOS-Chem model

142 GEOS-Chem (v13.4.0) model was employed to estimate O_3 and OH radical concentrations
143 during Jan. 1-Dec. 31 in 2019. This model comprises of a complex chemistry mechanism of



144 tropospheric NO_x-VOC-O₃-aerosol (Park et al., 2004). This model was driven by MERRA2
145 meteorological parameters (Hamal et al., 2020; Koster et al., 2020; Qiu et al., 2020). A global
146 simulation was conducted at a spatial resolution of 2 × 2.5° resolution (Qiu et al., 2020; Weagle et
147 al., 2018; Zhang et al., 2021a). The historical multi-sector anthropogenic emission dataset was
148 downloaded from Community Emissions Data System (Hoesly et al., 2018). Natural emissions
149 including wildfire, soil emission, and lightning emissions were also incorporated into the GEOS-
150 Chem model. Wildfire emissions derived from Global Fire Emissions Database (GFED) were used
151 for simulations (Chen et al., 2023). The lightning NO_x emission was collected from
152 http://geoschemdata.wustl.edu/ExtData/HEMCO/OFFLINE_LIGHTNING/v2020-03/MERRA2/
153 (Murray et al., 2012).

154 **3 Results and discussions**

155 3.1 The chemical compositions of PAHs and their derivatives in the atmosphere

156 The concentrations of 18 PAHs, 11 OPAHs, 9 RPAHs, and 7 NPAHs in 33 samples were
157 determined. The average concentrations of ΣPAHs, ΣOPAHs, ΣRPAHs, and ΣNPAHs were 157±98,
158 1920±1250, 12.1±9.5, and 3.0±1.6 pg/m³, respectively. The total concentrations of PAHs and their
159 derivatives in the marine aerosols (Pacific and Antarctic Ocean (AO)) were significantly lower than
160 those in urban regions such as Harbin (86.9 ng/m³) (Ma et al., 2020), Augsburg (1.3 ng/m³)
161 (Pietrogrande et al., 2011), and Southeastern Florida (3.0 ng/m³) (Sevimoglu and Rogge, 2016).
162 However, the PAHs concentration in our study was comparable to those in some remote regions.
163 For instance, Cabrerizo et al. (2014) found that the total concentration of 18 particulate PAHs over
164 AO ranged from 0.03 to 4.2 ng/m³. Later on, Zhang et al. (2022) reported that the 15 PAHs in PM_{2.5}
165 across Pacific and AO ranged from 0.11 to 1.2 ng/m³. Very recently, Van Overmeiren et al. (2024)
166 revealed that the total concentrations of 15 PAHs in PM_{2.5} in Antarctic was only 1.5 pg/m³, which
167 was even much lower than the result in our study. The large gaps for PAH concentrations between
168 remote ocean (polar region) and urban regions might be associated with the intensity of
169 anthropogenic emission (Shen et al., 2013; Zhang and Tao, 2009). Although the total concentration
170 could provide the overall picture of PAHs in the global marine boundary layer, the specific
171 compounds in PAHs also varied greatly.

172 Among all of the PAHs, the BbF showed the highest level (26.8±10.4 pg/m³), followed by Ace



173 (18.4±9.8 pg/m³), Fluoran (16.3±8.4 pg/m³), and the lowest one was Acy (0.12±0.05 pg/m³) (Figure
174 2). Overall, the PAHs in the global marine aerosols were dominated by 3-5 ring components (~83%),
175 which was in agreement with the result in Pacific and Indian Ocean observed by Zhang et al. (2022).
176 It was reported that Fluoran, Acy, and Ace were often sourced from biomass or coke burning (Zhang
177 et al., 2021c), while BbF was generally enriched in the production of wood and coal combustion (Li
178 et al., 2022), indicating the marine aerosols could be influenced by the solid fuel burning.

179 Among all of the OPAHs, 1-Naphthaldehyd showed the highest concentration (852±406 pg/m³),
180 followed by 1,4-Chysenequione (787±386 pg/m³), Ancenaphthenaquinone (133±75 pg/m³),
181 Anthraquinone (58±31 pg/m³), and the lowest one was 5,12-Naphthacenequione (1.49±0.64 pg/m³).
182 In general, the absolute concentrations of OPAHs were comparable or slightly lower than those of
183 PAHs especially in some high latitude sites. Nevertheless, the OPAHs concentrations in our study
184 were markedly higher than PAHs levels ($p < 0.01$). It was well known that OPAHs was often
185 released from incomplete combustion or generated from photochemical reactions of O₃, OH, and
186 NO₃ radicals with PAHs (Zhang et al., 2022). The higher concentrations of O₃ and OH radicals over
187 tropical oceans might largely promote the PAH oxidation (Zhang et al., 2022). For RPAHs, 1,3-
188 Dimethylnaphthalene (4.47±2.64 pg/m³) and 2-Methylnaphthalene (4.38±2.42 pg/m³) accounted for
189 the major fractions (73%) of RPAHs, while the concentrations of other species were relatively low.
190 Wietzorek et al. (2022) confirmed the chemical compositions of RPAHs in Middle East Seas
191 displayed similar patterns with our study. The NPAHs in the marine aerosols were also dominated
192 by 2-Nitronaphthalene (2.2±1.1 pg/m³) and 5-Nitroacenaphthene (2.0±0.7 pg/m³), while the
193 contributions of other species were negligible.

194 3.2 The spatial variations of particulate PAHs derivatives and key meteorological factors

195 To reveal the spatial variations of atmospheric PAHs and the derivatives, all of the sampling
196 sites were divided into five groups (regions): East China Sea (ECS), Western Pacific (WP),
197 Bismarck Sea (BS), Eastern Australia Sea (EAS), and AO. The PAHs concentrations followed the
198 order of WP (447±228 pg/m³) > ECS (195 pg/m³) > AO (111±91 pg/m³) > EAS (104±88 pg/m³) >
199 BS (17±12 pg/m³) (Figure 3). Based on Mann-Whitney test, the PAHs concentrations in WP were
200 significantly higher than those in other oceans ($p < 0.05$). High levels of PAHs in WP are closely
201 linked with the high coverage of continent-affected regions such as Southeast Asian and East Asian



202 countries. AO showed the lower PAHs concentrations because the sea was far away from continental
203 sources. In general, PAH levels in the remote marine atmosphere appear to be affected by long-
204 range transport and air-seawater exchange, whereas local anthropogenic emission might be
205 responsible for the ambient PAHs near the continent. For AO, the Antarctic continent lacks of
206 anthropogenic activity, and thus it leads to the lower PAHs levels in the atmosphere of AO. It should
207 be noted that both of EAS and BS were close to Australia, while the PAHs concentrations in these
208 seas were even lower than those in AO. It was assumed that Australia possesses very low
209 anthropogenic PAH emission ($< 10 \mu\text{g}/\text{km}^2$) compared with many other continents (Shen et al.,
210 2013). Although the total PAHs showed remarkably higher concentrations in ECS and WP, all of
211 the congeners did not show the same spatial variations with the total PAHs level. For instance,
212 Fluoran, Pyr, BeP, and BaP levels in AO were even higher than those in ECS and BbF level in EAS
213 was much higher than those in ECS. It was well documented that Pyr, BeP, and BaP were mainly
214 derived from engine combustion emissions (Van Overmeiren et al., 2024), indicating that the marine
215 aerosols in AO were often influenced by the shipping emission. BbF generally originated from wood
216 burning (Zhang et al., 2022a), and wildfire often occurred in the summer and autumn of Australia
217 (Haque et al., 2021), which might elevate the BbF concentration in the marine aerosols along
218 Australia. The simulated wildfire-related ambient benzene concentration via GEOS-Chem model
219 (Figure S2) was utilized to establish the relationship with the ambient BbF level in the aerosols, and
220 the correlation coefficient reached 0.52 ($p < 0.05$). The result confirmed that local wildfire in
221 Australia largely increased BbF concentration in the marine aerosol.

222 The total OPAHs also exhibited marked spatial variations with the highest concentrations in
223 WP ($3328 \pm 1846 \text{ pg}/\text{m}^3$), followed by EAS ($2675 \pm 1452 \text{ pg}/\text{m}^3$), ECS ($2506 \text{ pg}/\text{m}^3$), AO (1447 ± 865
224 pg/m^3), and the lowest one in BS ($897 \pm 544 \text{ pg}/\text{m}^3$). Different from the spatial distribution of parent
225 PAHs, OPAHs levels in EAS were much higher than those in AO and BS. It was widely
226 acknowledged that OPAHs were mainly derived from the secondary formation of parent PAH and
227 O_3 and OH radicals (Ambade et al., 2023). It was assumed that both of O_3 and OH radicals were
228 higher in the tropical oceans compared with the temperate and southern oceans based on GEOS-
229 Chem model (Figure S3). The correlation analysis also suggested that the OPAHs concentrations
230 displayed good relationship with O_3 level ($r = 0.55$, $p < 0.05$). In addition, the ratios of OPAH/PAH



231 in ECS, WP, BS, EAS, and AO were 13, 7, 53, 26, and 13, respectively. We could find that the
232 oxidation capacity of PAH in BS and EAS was much higher compared with other oceans, though
233 the primary emission of PAH in BS was relatively low. All of these results demonstrated that the
234 strong oxidation capacity of O₃ and OH radical promoted the higher OPAHs concentrations. Most
235 of the OPAH species displayed the similar spatial variations with the total OPAHs concentrations,
236 while few components such as 1-Naphthaldehyd, Ancenaphthenaquinone, and 6H-
237 Benzo(cd)pyrene-6-one levels in ECS were still higher than those in EAS. It might be linked with
238 the emission intensity of their precursors.

239 Both of RPAHs and NPAHs showed the higher levels in ECS (20 and 3.6 pg/m³) and WP
240 (22±13 and 3.0±1.2 pg/m³), which were significantly higher than those in other seas. Among all of
241 the species of RPAHs and NPAHs, 1-Methylnaphthalene and 2-Nitronaphthalene exhibited
242 significantly higher concentrations in ECS (1.61 and 3.61 pg/m³) and WP (2.1±1.3 and 2.8±1.1
243 pg/m³) compared with other regions (Figure S4 and S5) (*p* < 0.05). It was well documented that
244 both of these species were derived from diesel vehicle emission. Southeast Asia and East Asia
245 showed the higher diesel vehicle emission of parent PAHs compared with Australia and some
246 countries in South hemisphere (Shen et al., 2013).

247 Besides, some key meteorological factors including 2-m air temperature (T), 2-m dewpoint
248 temperature (Dew), precipitation (Prec), and wind speed (WS) were also selected to assess their
249 impacts on PAH derivatives (Figure 4). The result suggested that most of PAH derivatives showed
250 significant negative correlation with nearly all of the meteorological parameters. Among all of the
251 meteorological parameters, WS showed the highest correlation coefficients with all of the PAH
252 derivatives, indicating that dilution and diffusion conditions significantly affected their fate because
253 most of these compounds showed relatively long lifetime. Besides, T also showed the higher
254 negative correlation with PAH derivatives because the gas-particle partitioning of PAHs was mainly
255 controlled by the air temperature (Li et al., 2020; Wang et al., 2019b). High air temperature usually
256 suppresses gaseous to particulate sorption of PAH derivatives to marine aerosols, and compound-
257 dependent adsorption kinetics in the atmosphere (Andreae, 1983; Gustafson and Dickhut, 1996;
258 Wang et al., 2019a). Although rainfall washout might be an important pathway for PAH decrease,
259 the correlation coefficients of Prec and PAH derivatives were slightly lower than other



260 meteorological factors. It was assumed that the sampling period showed less rainfall events, and
261 thus the PAH derivatives were not sensitive to Prec. Compared with other PAH derivatives, RPAHs
262 showed low correlation coefficient with meteorological parameters.

263 3.3 Source apportionment of parent PAH and derivatives

264 The diagnostic ratio between PAHs has been widely utilized to identify the major sources of
265 particulate PAHs. Based on previous studies, the Fluoran/(Fluoran +Pyr) ratio could be applied to
266 distinguish the potential sources. The ratios less than 0.4, 0.4-0.5, and greater than 0.5 could be
267 treated to be petrogenic source, petroleum combustion or biomass burning, and the coal combustion,
268 respectively (Yunker et al., 2002; Zhang et al., 2021a). In our study, the Fluoran/(Fluoran +Pyr) ratio
269 in nearly all of the regions except AO (0.46) were higher than 0.5, indicating the impact of coal
270 combustion on marine aerosols in most regions in Northern Hemisphere and tropical regions. The
271 geochemical index method shows some uncertainties, and thus it is necessary to employ more
272 diagnostic ratios to enhance the reliability. BaP/BghiP ratio was also widely applied to separate the
273 sources of vehicle emission (≤ 0.6) and coal burning (> 0.6). Both of BS (0.90) and EAS (0.84)
274 showed the higher BaP/BghiP ratios, indicating the important impact of coal combustion on the
275 local marine aerosols (Katsoyiannis et al., 2007). However, the ratio in ECS was much lower than
276 0.6, indicating that the vehicle or shipping emission also plays a unignorable role on the local
277 aerosols. Meanwhile, the BaP/(BaP+CT) ratios in ECS and WP reached 0.09 and 0.31, respectively.
278 The result fills in the domain derived from diesel emission, which further supported the inference
279 that the marine aerosols in both of ECS and WP were significantly affected by diesel emission (Ma
280 et al., 2020). For AO, all of the diagnostic ratios suggested that the oceans were mainly affected by
281 shipping emission and wood burning.

282 Although the geochemical index method could identify the potential sources of PAH species,
283 the contributions of multiple sources to PAHs and their derivatives still remained unknown.
284 Therefore, positive matrix factorization (version PMF 5.0) was utilized to determine more source
285 information of PAH species. After 30 runs, the optimal three factors with the lowest values of Q
286 (robust) and Q (true) were determined. Factor 1 (56%) possesses the higher loadings of Fluoran,
287 BaA, CT, BeP, BaP, and 1-Methylnaphthalene (Figure 5). It was well known that Fluoran and BaA
288 were typical indicators for coal combustion (Wang et al., 2016). Meanwhile, BeP, BaP, and 1-



289 Methylanthalene were often derived from shipping emission (Li et al., 2022). Therefore, factor 1
290 could be defined as the mixed source of coal burning and engine combustion emission. Factor 2
291 (30%) shows a high correlation with LMW PAHs such as Nap, Flu, Phe, Ant, BbF. It was well
292 documented that these LMW PAH species mainly originated from wood and biomass burning (Chen
293 et al., 2022; Zhang et al., 2021a; Zhang et al., 2020). Factor 3 (14%) is characterized by medium
294 and high contributions of 5,12-Naphthacenequinone, 1,6,7-Trimethylnaphthalene, and 2-
295 Nitronaphthalene. Many previous studies have confirmed that the photochemical reaction involving
296 NO₂ initiated by OH radicals was highly effective for the production of 2-Nitronaphthalene in PM_{2.5}
297 (Arey et al., 1990; Atkinson et al., 1990). Hence, the factor could be treated to be the secondary
298 formation.

299 **4 Conclusions and implications**

300 In summary, our study verifies the ubiquitous occurrence of PAHs and their derivatives in the
301 aerosols of the Western Pacific (WP), Bismarck Sea (BS), East Australian Sea (EAS), and even the
302 Antarctic Ocean (AO). The highest PAH concentrations in marine aerosols were observed in WP
303 (447±228 pg/m³), followed by the East China Sea (ECS) (195 pg/m³), AO (111±91 pg/m³), EAS
304 (104±88 pg/m³), and the lowest in BS (17±12 pg/m³). PAH derivatives (e.g., OPAHs, RPAHs, and
305 NPAHs) also showed higher concentrations in WP. The spatial characteristics of these components
306 were determined by precursor emissions and oxidation patterns (e.g., OH/NO₃ radicals, O₃).

307 For instance, the higher PAH and derivative concentrations observed in WP were primarily due
308 to higher anthropogenic emissions from coal and engine combustion. PAH concentrations in AO
309 were even higher than those in EAS and BS, while OPAH levels in EAS were much higher than
310 those in AO. It is widely acknowledged that OPAHs mainly originate from the secondary formation
311 of parent PAHs through reactions with O₃ and OH radicals. The concentrations of O₃ and OH
312 radicals are higher in tropical oceans compared to temperate and southern oceans.

313 Both of geochemical index methods and the PMF model suggested that PAHs and their
314 derivatives in global marine aerosols are controlled by three major sources: coal burning and engine
315 combustion emissions (56%), wood and biomass burning (30%), and secondary formation (14%).
316 Marine aerosols in ECS and WP were dominated by coal burning and engine combustion, while BS
317 and EAS were mainly influenced by wildfires and coal combustion. AO was significantly affected



318 by biomass burning and local shipping emissions.

319 However, this study has some limitations. Firstly, it focuses only on particle-phase PAHs and
320 derivatives, while gas-phase PAH species were not measured. Additionally, data on PAHs in
321 seawater were lacking. Future research should investigate gas-particle partitioning and the exchange
322 processes between air and seawater phases in the global marine environment. Moreover, our study
323 did not include cruise observations of marine aerosols in the Atlantic and Arctic Oceans. Future
324 studies should collect marine aerosols from all major oceans. Furthermore, measuring the
325 concentrations of PAHs and derivatives in marine aerosols over multiple years will help analyze the
326 impact of changes in anthropogenic emissions on these components, providing insight into their
327 spatial distribution and fate (formation or removal mechanisms).

328 **Acknowledgements**

329 This work was supported by the National Natural Science Foundation of China (42107113,
330 42276243), and the Fundamental Research Funds for the Central Universities. The authors are
331 grateful to the CHINARE members for their support and assistance in atmosphere sampling.

332 **Data Availability Statement**

333 The data presented in this study are available at the Zenodo data archive
334 <https://zenodo.org/records/14291911> (Li et al., 2024).

335 **Author Contributions**

336 Conceptualization: Rui Li, Xing Liu, and Guitao Shi; Data Curation: Yubing Shen, Yumeng Shao,
337 and Yining Gao; Formal analysis: Ziwei Yao, Qian Liu

338 **Competing interests**

339 The contact author has declared that none of the authors has any competing interests.

340



341 **References**

342 Ambade, B., Sethi, S.S., Chintalacheruvu, M.R. (2023) Distribution, risk assessment, and
343 source apportionment of polycyclic aromatic hydrocarbons (PAHs) using positive matrix
344 factorization (PMF) in urban soils of East India. *Environmental geochemistry and health* 45, 491-
345 505.

346 Andreae, M.O. (1983) Soot carbon and excess fine potassium: Long-range transport of
347 combustion-derived aerosols. *Science* 220, 1148-1151.

348 Arey, J., Atkinson, R., Aschmann, S.M., Schuetzle, D. (1990) Experimental investigation of
349 the atmospheric chemistry of 2-methyl-1-nitronaphthalene and a comparison of predicted nitroarene
350 concentrations with ambient air data. *Polycyclic Aromatic Compounds* 1, 33-50.

351 Atkinson, R., Arey, J., Zielinska, B., Aschmann, S.M. (1990) Kinetics and nitro-products of
352 the gas-phase OH and NO₃ radical-initiated reactions of naphthalene-d₈, Fluoranthene-d₁₀, and
353 pyrene. *International Journal of Chemical Kinetics* 22, 999-1014.

354 Bandowe, B.A.M., Meusel, H. (2017) Nitrated polycyclic aromatic hydrocarbons (nitro-PAHs)
355 in the environment—a review. *Science of the Total Environment* 581, 237-257.

356 Cabrerizo, A., Galbán-Malagón, C., Del Vento, S., Dachs, J. (2014) Sources and fate of
357 polycyclic aromatic hydrocarbons in the Antarctic and Southern Ocean atmosphere. *Global*
358 *Biogeochemical Cycles* 28, 1424-1436.

359 Chen, Y.-P., Zeng, Y., Guan, Y.-F., Huang, Y.-Q., Liu, Z., Xiang, K., Sun, Y.-X., Chen, S.-J.
360 (2022) Particle size-resolved emission characteristics of complex polycyclic aromatic hydrocarbon
361 (PAH) mixtures from various combustion sources. *Environmental Research* 214, 113840.

362 Gao, B., Wang, X.-M., Zhao, X.-Y., Ding, X., Fu, X.-X., Zhang, Y.-L., He, Q.-F., Zhang, Z.,
363 Liu, T.-Y., Huang, Z.-Z. (2015) Source apportionment of atmospheric PAHs and their toxicity using
364 PMF: Impact of gas/particle partitioning. *Atmospheric Environment* 103, 114-120.

365 Gustafson, K.E., Dickhut, R.M. (1996) Particle/gas concentrations and distributions of PAHs
366 in the atmosphere of southern Chesapeake Bay. *Environmental science & technology* 31, 140-147.

367 Haque, M.K., Azad, M.A.K., Hossain, M.Y., Ahmed, T., Uddin, M., Hossain, M.M. (2021)
368 Wildfire in Australia during 2019-2020, Its impact on health, biodiversity and environment with
369 some proposals for risk management: a review. *Journal of Environmental Protection* 12, 391-414.



370 Jaeckels, J.M., Bae, M.-S., Schauer, J.J. (2007) Positive matrix factorization (PMF) analysis of
371 molecular marker measurements to quantify the sources of organic aerosols. *Environmental science
372 & technology* 41, 5763-5769.

373 Kang, M., Yang, F., Ren, H., Zhao, W., Zhao, Y., Li, L., Yan, Y., Zhang, Y., Lai, S., Zhang, Y.
374 (2017) Influence of continental organic aerosols to the marine atmosphere over the East China Sea:
375 Insights from lipids, PAHs and phthalates. *Science of the Total Environment* 607, 339-350.

376 Katsoyiannis, A., Terzi, E., Cai, Q.-Y. (2007) On the use of PAH molecular diagnostic ratios in
377 sewage sludge for the understanding of the PAH sources. Is this use appropriate? *Chemosphere* 69,
378 1337-1339.

379 Kovacic, P., Somanathan, R. (2014) Nitroaromatic compounds: Environmental toxicity,
380 carcinogenicity, mutagenicity, therapy and mechanism. *Journal of Applied Toxicology* 34, 810-824.

381 Li, B., Zhou, S., Wang, T., Zhou, Y., Ge, L., Liao, H. (2020) Spatio-temporal distribution and
382 influencing factors of atmospheric polycyclic aromatic hydrocarbons in the Yangtze River Delta.
383 *Journal of Cleaner Production* 267, 122049.

384 Li, C., Li, Z., Wang, H. (2023) Characterization and risk assessment of polycyclic aromatic
385 hydrocarbons (PAHs) pollution in particulate matter in rural residential environments in China-A
386 review. *Sustainable Cities and Society*, 104690.

387 Li, D., Zhao, Y., Du, W., Zhang, Y., Chen, Y., Lei, Y., Wu, C., Wang, G. (2022) Characterization
388 of PM_{2.5}-bound parent and oxygenated PAHs in three cities under the implementation of Clean Air
389 Action in Northern China. *Atmospheric Research* 267, 105932.

390 Li, R., Hua, P., Krebs, P. (2021a) Global trends and drivers in consumption-and income-based
391 emissions of polycyclic aromatic hydrocarbons. *Environmental science & technology* 56, 131-144.

392 Li, R., Shen, Y., Shao, Y., Gao, Y., Yao, Z., Liu, Q., Liu, X., Shi, G. (2024) Measurement Report:
393 Polycyclic aromatic hydrocarbons (PAHs) and their alkylated (RPAHs), nitrated (NPAHs) and
394 oxygenated (OPAHs) derivatives in the global marine atmosphere: occurrence, spatial variations,
395 and source apportionment. *Atmospheric Chemistry and Physics*.

396 Li, Y., Liu, M., Hou, L., Li, X., Yin, G., Sun, P., Yang, J., Wei, X., He, Y., Zheng, D. (2021b)
397 Geographical distribution of polycyclic aromatic hydrocarbons in estuarine sediments over China:
398 Human impacts and source apportionment. *Science of the Total Environment* 768, 145279.



- 399 Lian, L., Huang, T., Ke, X., Ling, Z., Jiang, W., Wang, Z., Song, S., Li, J., Zhao, Y., Gao, H.
400 (2021) Globalization-driven industry relocation significantly reduces arctic PAH contamination.
401 *Environmental science & technology* 56, 145-154.
- 402 Ma, L., Li, B., Liu, Y., Sun, X., Fu, D., Sun, S., Thapa, S., Geng, J., Qi, H., Zhang, A. (2020)
403 Characterization, sources and risk assessment of PM_{2.5}-bound polycyclic aromatic hydrocarbons
404 (PAHs) and nitrated PAHs (NPAHs) in Harbin, a cold city in Northern China. *Journal of Cleaner
405 Production* 264, 121673.
- 406 Neroda, A.S., Goncharova, A.A., Mishukov, V.F. (2020) PAHs in the atmospheric aerosols and
407 seawater in the North–West Pacific Ocean and Sea of Japan. *Atmospheric Environment* 222, 117117.
- 408 Pegoraro, C.N., Quiroga, S.L., Montejano, H.A., Rimondino, G.N., Argüello, G.A., Chiappero,
409 M.S. (2020) Assessing polycyclic aromatic hydrocarbons in the marine atmosphere on a transect
410 across the Southwest Atlantic Ocean. *Atmospheric Pollution Research* 11, 1035-1041.
- 411 Pietrogrande, M.C., Abbaszade, G., Schnelle-Kreis, J., Bacco, D., Mercuriali, M.,
412 Zimmermann, R. (2011) Seasonal variation and source estimation of organic compounds in urban
413 aerosol of Augsburg, Germany. *Environmental pollution* 159, 1861-1868.
- 414 Sevimglu, O., Rogge, W.F. (2016) Seasonal size-segregated PM₁₀ and PAH concentrations
415 in a rural area of sugarcane agriculture versus a coastal urban area in Southeastern Florida, USA.
416 *Particuology* 28, 52-59.
- 417 Sharma, S., Mandal, T., Jain, S., Saraswati, Sharma, A., Saxena, M. (2016) Source
418 apportionment of PM_{2.5} in Delhi, India using PMF model. *Bulletin of environmental contamination
419 and toxicology* 97, 286-293.
- 420 Shen, H., Huang, Y., Wang, R., Zhu, D., Li, W., Shen, G., Wang, B., Zhang, Y., Chen, Y., Lu,
421 Y. (2013) Global atmospheric emissions of polycyclic aromatic hydrocarbons from 1960 to 2008
422 and future predictions. *Environmental science & technology* 47, 6415-6424.
- 423 Taghvaei, S., Sowlat, M.H., Mousavi, A., Hassanvand, M.S., Yunesian, M., Naddafi, K.,
424 Sioutas, C. (2018) Source apportionment of ambient PM_{2.5} in two locations in central Tehran using
425 the Positive Matrix Factorization (PMF) model. *Science of the Total Environment* 628, 672-686.
- 426 Van Overmeiren, P., Demeestere, K., De Wispelaere, P., Gili, S., Mangold, A., De Causmaecker,
427 K., Mattielli, N., Delcloo, A., Langenhove, H.V., Walgraeve, C. (2024) Four Years of Active



428 Sampling and Measurement of Atmospheric Polycyclic Aromatic Hydrocarbons and Oxygenated
429 Polycyclic Aromatic Hydrocarbons in Dronning Maud Land, East Antarctica. *Environmental*
430 *science & technology* 58, 1577-1588.

431 Wang, J., Ho, S.S.H., Huang, R., Gao, M., Liu, S., Zhao, S., Cao, J., Wang, G., Shen, Z., Han,
432 Y. (2016) Characterization of parent and oxygenated-polycyclic aromatic hydrocarbons (PAHs) in
433 Xi'an, China during heating period: An investigation of spatial distribution and transformation.
434 *Chemosphere* 159, 367-377.

435 Wang, L., Dong, S., Liu, M., Tao, W., Xiao, B., Zhang, S., Zhang, P., Li, X. (2019a) Polycyclic
436 aromatic hydrocarbons in atmospheric PM_{2.5} and PM₁₀ in the semi-arid city of Xi'an, Northwest
437 China: Seasonal variations, sources, health risks, and relationships with meteorological factors.
438 *Atmospheric Research* 229, 60-73.

439 Wang, Y., Zhang, Q., Zhang, Y., Zhao, H., Tan, F., Wu, X., Chen, J. (2019b) Source
440 apportionment of polycyclic aromatic hydrocarbons (PAHs) in the air of Dalian, China: Correlations
441 with six criteria air pollutants and meteorological conditions. *Chemosphere* 216, 516-523.

442 Wei, C., Bandowe, B.A.M., Han, Y., Cao, J., Watson, J.G., Chow, J.C., Wilcke, W. (2021)
443 Polycyclic aromatic compounds (PAHs, oxygenated PAHs, nitrated PAHs, and azaarenes) in air
444 from four climate zones of China: Occurrence, gas/particle partitioning, and health risks. *Science of*
445 *the Total Environment* 786, 147234.

446 Wietzorek, M., Kyprianou, M., Musa Bandowe, B.A., Celik, S., Crowley, J.N., Drewnick, F.,
447 Eger, P., Friedrich, N., Iakovides, M., Kukučka, P. (2022) Polycyclic aromatic hydrocarbons (PAHs)
448 and their alkylated, nitrated and oxygenated derivatives in the atmosphere over the Mediterranean
449 and Middle East seas. *Atmospheric Chemistry and Physics* 22, 8739-8766.

450 Yan, Y., He, Q., Guo, L., Li, H., Zhang, H., Shao, M., Wang, Y. (2017) Source apportionment
451 and toxicity of atmospheric polycyclic aromatic hydrocarbons by PMF: Quantifying the influence
452 of coal usage in Taiyuan, China. *Atmospheric Research* 193, 50-59.

453 Yunker, M.B., Macdonald, R.W., Vingarzan, R., Mitchell, R.H., Goyette, D., Sylvestre, S.
454 (2002) PAHs in the Fraser River basin: a critical appraisal of PAH ratios as indicators of PAH source
455 and composition. *Organic geochemistry* 33, 489-515.

456 Zhang, L., Yang, L., Bi, J., Liu, Y., Toriba, A., Hayakawa, K., Nagao, S., Tang, N. (2021a)



457 Characteristics and unique sources of polycyclic aromatic hydrocarbons and nitro-polycyclic
458 aromatic hydrocarbons in PM_{2.5} at a highland background site in northwestern China ☆ .
459 Environmental pollution 274, 116527.

460 Zhang, L., Yang, L., Zhou, Q., Zhang, X., Xing, W., Wei, Y., Hu, M., Zhao, L., Toriba, A.,
461 Hayakawa, K. (2020) Size distribution of particulate polycyclic aromatic hydrocarbons in fresh
462 combustion smoke and ambient air: A review. Journal of Environmental Sciences 88, 370-384.

463 Zhang, P., Zhou, Y., Chen, Y., Yu, M., Xia, Z. (2023) Construction of an atmospheric PAH
464 emission inventory and health risk assessment in Jiangsu, China. Air Quality, Atmosphere & Health
465 16, 629-640.

466 Zhang, R., Han, M., Yu, K., Kang, Y., Wang, Y., Huang, X., Li, J., Yang, Y. (2021b) Distribution,
467 fate and sources of polycyclic aromatic hydrocarbons (PAHs) in atmosphere and surface water of
468 multiple coral reef regions from the South China Sea: A case study in spring-summer. Journal of
469 hazardous materials 412, 125214.

470 Zhang, X., Zhang, Z.-F., Zhang, X., Zhu, F.-J., Li, Y.-F., Cai, M., Kallenborn, R. (2022a)
471 Polycyclic aromatic hydrocarbons in the marine atmosphere from the Western Pacific to the
472 Southern Ocean: Spatial variability, Gas/particle partitioning, and source apportionment.
473 Environmental science & technology 56, 6253-6261.

474 Zhang, Y., Shen, Z., Sun, J., Zhang, L., Zhang, B., Zou, H., Zhang, T., Ho, S.S.H., Chang, X.,
475 Xu, H. (2021c) Parent, alkylated, oxygenated and nitrated polycyclic aromatic hydrocarbons in PM_{2.5}
476 emitted from residential biomass burning and coal combustion: A novel database of 14 heating
477 scenarios. Environmental pollution 268, 115881.

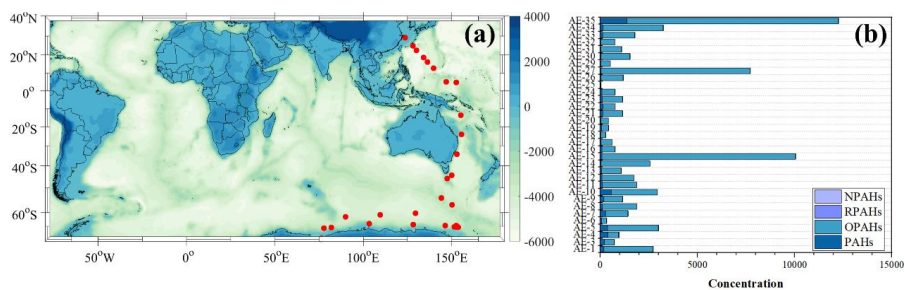
478 Zhang, Y., Tao, S. (2009) Global atmospheric emission inventory of polycyclic aromatic
479 hydrocarbons (PAHs) for 2004. Atmospheric Environment 43, 812-819.

480 Zhang, Z.-F., Chen, J.-C., Zhao, Y.-X., Wang, L., Teng, Y.-Q., Cai, M.-H., Zhao, Y.-H.,
481 Nikolaev, A., Li, Y.-F. (2022b) Determination of 123 polycyclic aromatic hydrocarbons and their
482 derivatives in atmospheric samples. Chemosphere 296, 134025.

483 Zimmermann, K., Jariyasopit, N., Massey Simonich, S.L., Tao, S., Atkinson, R., Arey, J. (2013)
484 Formation of nitro-PAHs from the heterogeneous reaction of ambient particle-bound PAHs with
485 N₂O₅/NO₃/NO₂. Environmental science & technology 47, 8434-8442.



488 **Figure 1** The sampling sites during the cruise from Shanghai to Antarctic (red dots) (a). The total
489 concentrations (Unit: pg/m^3) of PAHs, OPAHs, RPAHs, and NPAHs for all of the samples (from
490 AE-1 to AE-35) (b). The indicators from AE-1 to AE-35 represent the collected aerosol samples in
491 the global marine.

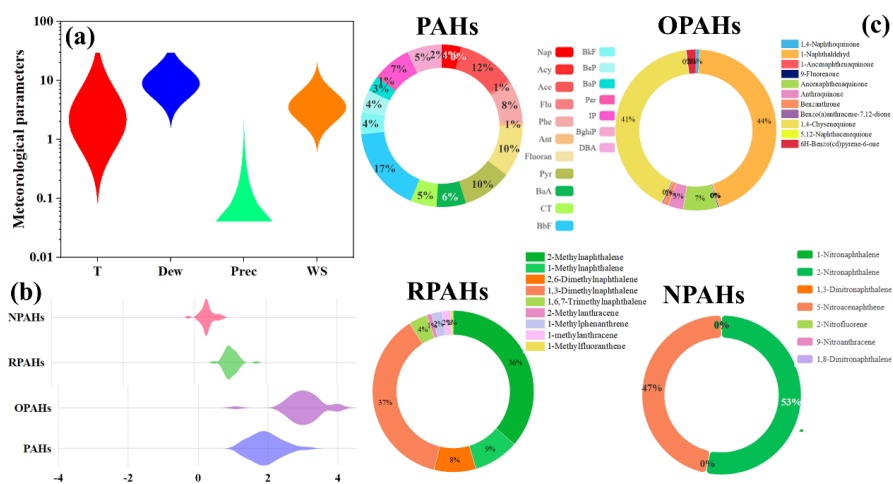


492

493



494 **Figure 2** The average meteorological parameters during the cruise (a). T, Dew, Prec, and WS denote
 495 2-m air temperature (Unit: °C), dewpoint temperature (Unit: °C), precipitation (mm), and wind
 496 speed (m/s), respectively. The average concentrations (log₁₀ (concentration), Unit: pg/m³) of PAHs,
 497 OPAHs, RPAHs, and NPAHs for all of the samples (b). The contribution ratios of species in PAHs,
 498 OPAHs, RPAHs, and NPAHs (Unit: %) (c).

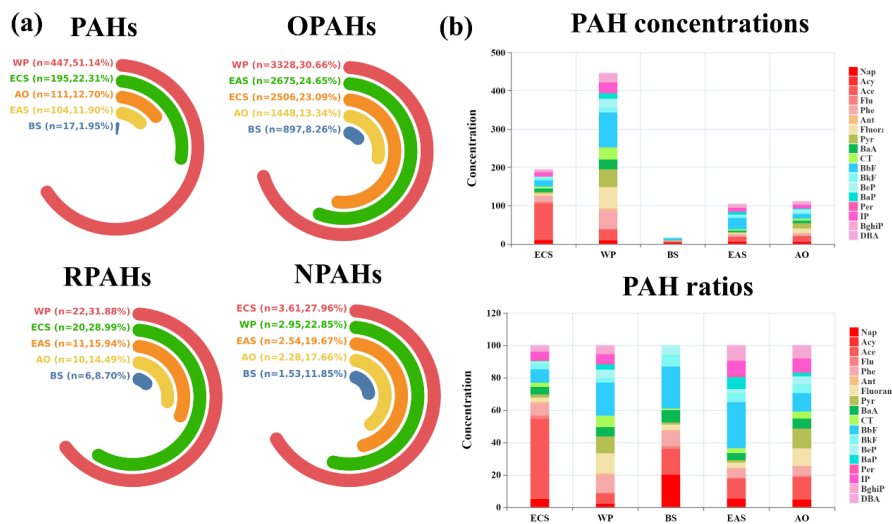


499

500



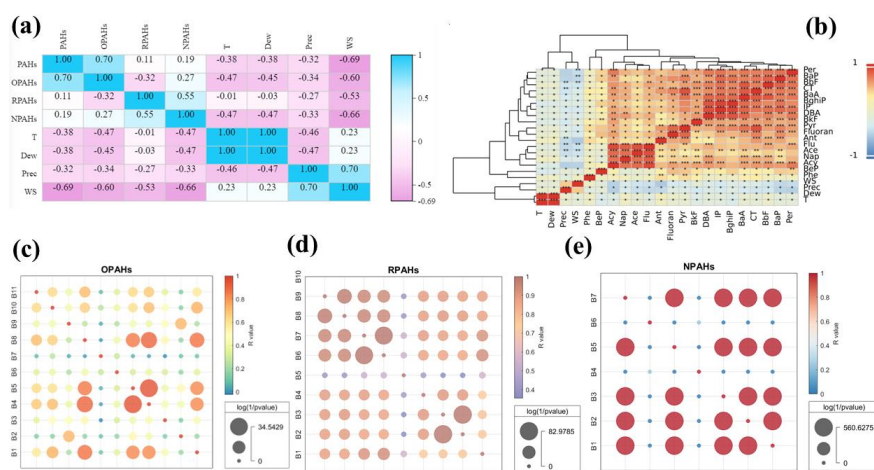
501 **Figure 3** The spatial variations of PAHs and derivatives in the marine aerosols (e.g., n means the
 502 average concentration of PAHs and derivatives, and the ratio (%) denotes the quotient of PAHs
 503 concentrations in each region and the total concentrations in all of five regions (a). The spatial
 504 distributions of PAH species (Unit: pg/m³) in the global marine aerosols (b).



505



506 **Figure 4** The correlation of PAHs, OPAHs, RPAHs, and NAPHs and meteorological parameters.
 507 The correlation of PAH species and meteorological factors (b). The correlation coefficients and log
 508 (1/p values) of OPAH species (c). A1, A2, A3, A4, A5, A6, A7, A8, A9, A10, and A11 in (c) represent
 509 1,4-Naphthoquinone, 1-Naphthaldehyd, 1-Ancenaphthenaquinone, 9-Fluorenone,
 510 Ancenaphthenaquinone, Anthraquinone, Benzanthrone, Benzo(a)anthracene-7,12-dione, 1,4-
 511 Chysenequione, 5,12-Naphthacenequione, and 6H-Benzo(cd)pyrene-6-one, respectively. The
 512 correlation coefficients and log (1/p values) of RPAH species (d). A1, A2, A3, A4, A5, A6, A7, A8,
 513 and A9 in (d) denote 2-Methylnaphthalene, 1-Methylnaphthalene, 2,6-Dimethylnaphthalene, 1,3-
 514 Dimethylnaphthalene, 1,6,7-Trimethylnaphthalene, 2-Methylanthracene, 1-Methylphenanthrene, 1-
 515 methylanthracene, 1-Methylfluoranthene, respectively. The correlation coefficients and log (1/p
 516 values) of NPAH species (e). A1, A2, A3, A4, A5, A6, and A7 in (e) reflects 1-Nitronaphthalene, 2-
 517 Nitronaphthalene, 1,3-Dinitronaphthalene, 5-Nitroacenaphthene, 2-Nitrofluorene, 9-
 518 Nitroanthracene, 1,8-Dinitronaphthalene, respectively.

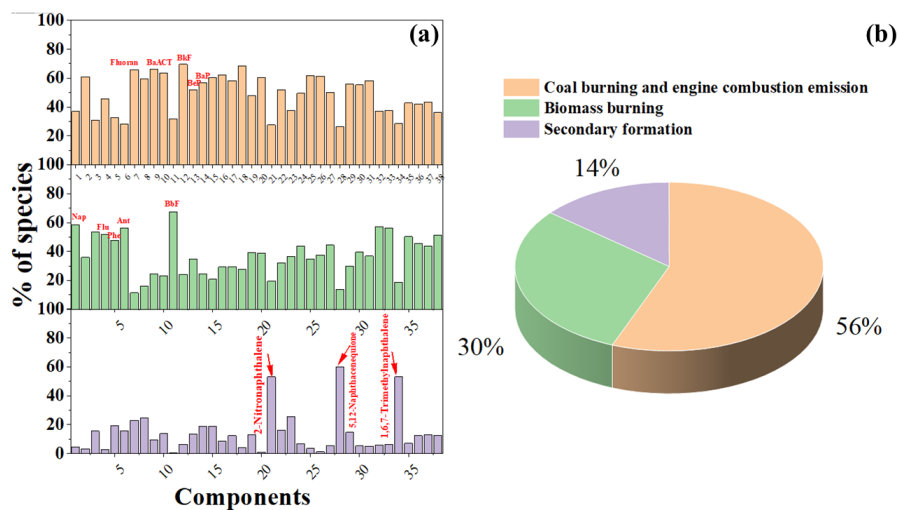


519

520



521 **Figure 5** The factor profiles (% of species) resolved from PMF analysis (a). Source contributions
 522 of three factors to the total parent PAHs and derivatives in PM_{2.5} at the marine atmosphere (b). The
 523 number from 1 to 38 denote Nap, Acy, Ace, Flu, Phe, Ant, Fluoran, Pyr, BaA, CT, BbF, BkF, BeP,
 524 BaP, Per, IP, BghiP, DBA, 1,4-Naphthoquinone, 1-Naphthaldehyd, 2-Nitronaphthalene, 1-
 525 Ancenaphthenaquinone, 9-Fluorenone, Ancenaphthenaquinone, Anthraquinone, Benzanthrone,
 526 Benzo(a)anthracene-7,12-dione, 1,4-Chysenequione, 5,12-Naphthacenequione, 6H-
 527 Benzo(cd)pyrene-6-one, 2-Methylnaphthalene, 1-Methylnaphthalene, 2,6-Dimethylnaphthalene,
 528 1,3-Dimethylnaphthalene, 1,6,7-Trimethylnaphthalene, 2-Methylantracene, 1-
 529 Methylphenanthrene, and 1-methylantracene, respectively.



530